

**Characterization of Anomalous Flow and Phase Behavior in a Langmuir Monolayer
of 2-hydroxy-tetracosanoic acid**

Michael Twardos*, Michael Dennin*, and Gerald Brezesinski[#]

**Department of Physics and Astronomy and Institute for Interfacial and Surface Science
University of California at Irvine, Irvine, CA 92697-4575*

*# Max Planck Institute of Colloids and Interfaces
Research Campus Golm, Am Muehlenberg 1, D-14476 Potsdam, Germany*

Langmuir monolayers of long chain fatty acids display a wide range of interesting flow and phase behavior, but the correlation between these behaviors varies. In this paper, we report two interesting behaviors in a Langmuir monolayer of 2-hydroxy-tetracosanoic acid (2-OH TCA): phase coexistence between the L_{2h} and $L_{2'}$ phases over a large pressure range and a peak in the viscosity and elastic modulus of the material as a function of pressure. The two behaviors are confirmed over a range of temperatures for which the location of the undistorted lattice appears to vary relative to the range of coexistence for the two phases. Evidence for a correlation between the phase behavior and the peak in the mechanical properties is presented.

1. Introduction

Recent studies of the flow behavior of Langmuir monolayers have revealed a number of surprising results. Among these are unusual velocity profiles¹⁻³, interesting flow alignment⁴⁻⁶, and anomalous pressure dependence of the viscosity⁷⁻¹⁰. The variety of flow behavior in Langmuir monolayers is closely related to the richness of their phase diagrams^{11,12}. Langmuir monolayers consist of amphiphilic molecules that are confined to the air-water interface. In addition to the two-dimensional gas, liquid, and solid phases, they exhibit a wide range of two-dimensional liquid crystalline (LC) phases^{11,12}. The renewed interest in monolayer flow behavior has focused on these LC phases, and a range of techniques have been used to study flow behavior¹³. One of the clear issues raised by many of the recent measurements is the impact on the bulk flow behavior of structure on the mesoscopic level in the form of domains¹⁴ and of molecular interactions on the microscopic level¹⁵. Because of their two-dimensional nature, Langmuir monolayers present a unique opportunity to study the relative importance of the mesoscopic and microscopic influences on flow. The observation of an anomalous pressure peak is one example of this issue^{8,9}.

It was very surprising to find that the L_2 phase of heneicosanoic acid (C21) exhibits a peak in the imaginary part of the complex shear modulus⁸, G'' , and the viscosity⁹, η , as a function of pressure. An intriguing aspect of this anomalous behavior is that it is correlated with the symmetry of the underlying hexatic lattice of the monolayer, and not with a phase transition⁸. As the film is compressed in the L_2 phase, the shape of the lattice changes from a “broad” hexagon to a “tall” hexagon. During this continuous structural change, there is an intermediate pressure Π_{hex} at which the lattice is

exactly hexagonal and G'' reaches a maximum within the phase. However, it is not known how this could *explain* the peak in viscosity, and if this peak is truly due to changes on the microscopic scale. In contrast to the work with C21, work with fatty alcohols have shown a peak in the viscosity that is not correlated with any obvious changes in the underlying lattice^{7,10}. In this case, the peak is in the L_2' phase, and it was observed for situations where the high-pressure, untilted phase was the LS phase, which is known to have a very low viscosity^{7,10,16}. This peak was attributed to the reduction in tilt angle¹⁰. However, the L_2' phase of C21 has a similar reduction in tilt angle, but no corresponding peak in the viscosity⁸. In this case, the high-pressure, untilted phase is the S or CS phase. These two experiments suggest multiple microscopic mechanisms for a peak occurring in the mechanical response of a monolayer.

In this paper, we present the results of experimental measurements of the viscoelastic behavior of the fatty acid 2-hydroxy-tetracosanoic acid (2-OH TCA) and x-ray measurements of the monolayer structure. There are two surprising features of this system. First, as a function of surface pressure, there exists a peak in a number of different measures of the bulk flow properties. Second, the x-ray measurements reveal a relatively large range of surface pressure for which the L_{2h} and L_2' phases coexist. This coexistence is not evident in the isotherm measurements. An experimental challenge is determining the correlation between the peak in viscosity and the structure of the monolayer. One issue is whether or not the mechanism is related to the two previously observed mechanisms: reduction in tilt angle¹⁰ or structure of the underlying lattice⁸. Our observations rule out a correlation with the undistorted hexagonal lattice and strongly suggest that the peak is tied to the behavior of the tilt of the chains.

2. Experimental Section

We measure the mechanical properties of the system using a two dimensional Couette viscometer that is described in detail in Ref. 17. The apparatus consists of two concentric cylinders oriented vertically. Millipore filtered water with a resistivity of 18.2 M Ω cm is placed between the cylinders. Two different subphases were used for the rheological measurements. Pure water was used that had a pH of 5.6, and water maintained at a constant pH of 2.5 with the addition of HCl to prevent possible ionic contamination to the monolayer. The outer cylinder consists of 12 individual pieces that can be expanded and compressed between 6 and 12 cm to adjust the surface pressure. This barrier can be rotated in either direction at a constant angular speed in the range of 0.0005 rad/s to 0.1 rad/s. The inner cylinder is a Teflon rotor that contacts the film with a knife-edge. To avoid interference effects, an inner cylinder below the rotor used to create Couette flow was removed. In our measurements, the viscoelasticity of the monolayer was large enough that the monolayer is decoupled from the subphase^{1,18}. The rotor has a diameter of 3.84 cm and is suspended by a torsion wire with a torsion constant, $\kappa=370$ dyne cm/rad. A coil was attached to the pendulum and placed within a high frequency magnetic field. The induced voltage was used to determine the angle of the coil. The voltage is linearly proportional to the angle for small angle displacements. A constant current was also directed through the inner coil providing it with a constant magnetic dipole moment. This can be used to apply a stress on the inner rotor with a low frequency external magnetic field.

The 2-OH TCA was dissolved in chloroform for spreading on the surface. The solution was placed on the aqueous subphase with a microsyringe and allowed to relax

for 30 minutes before compression to facilitate the evaporation of the solvent. The subphase temperature was varied from 15.5 ± 0.1 to 30.0 ± 0.1 °C. One challenge for the experiments is that the 2-OH TCA is used as received. There is some systematic variation in the measured pressures for the phase transitions. Therefore, for comparisons between multiple samples, it is important to consider differences in pressure between two transitions, as well as the absolute value of the transitions.

We report on the complex shear modulus $G^*(\omega)$. This is measured by driving the torsion pendulum and measuring the response. The torsion pendulum can be driven at a fixed frequency, in the range 0.03 rad/s – 2 rad/s by an external magnetic field. The complex shear modulus is strongly amplitude dependent for large amplitudes⁸. Therefore, for all measurements reported here, the amplitude was kept small and constant at 10^{-3} rad. The amplitude of the sinusoidal response of the rotor and its phase relative to the driving torque were determined. From this, the complex shear modulus, $G^*(\omega)$, of the system is calculated. Alternatively, we also measured steady-state viscosity and the time-dependent “relaxation modulus”, $G(t)$ ¹⁹. This is done by applying a steady rate of strain to the system by rotating the outer cylinder. The stress induced by this is measured using the torsion pendulum. The results for these measurements revealed a peak at the same value of pressure as the complex shear modulus for any given monolayer that was studied.

Grazing incidence x-ray diffraction (GIXD) measurements were performed both on pure water and at a pH of 2.5 using the liquid surface diffractometer (beamline BW1) at HASYLAB, DESY, Hamburg, Germany. The Synchrotron beam was made monochromatic by a Beryllium (002) crystal. Experiments were performed at an angle of incidence of $0.85 * \alpha_c$ (α_c is the critical angle for total external reflection). A linear

position sensitive detector (PSD) (OED-100-M, Braun, Garching, Germany) with a vertical acceptance $0 < Q_z < 1.27 \text{ \AA}^{-1}$ was used for recording the diffracted intensity as a function of both the vertical (Q_z) and the horizontal (Q_{xy}) scattering vector components. The horizontal resolution of 0.008 \AA^{-1} was determined by a Soller collimator mounted in front of the PSD. The analysis of the in-plane diffraction data yields lattice spacings according to $d_{hk} = 2\pi / Q_{xy}^{hk}$. The in-plane and out-of-plane peak positions give information about the tilt angle and the tilt direction. For more information about the principles of GIXD for the study of two-dimensional condensed films at the air-liquid interface, we kindly refer to detailed reviews published recently^{12,20,21}.

3. Experimental Results

We probed the equilibrium phase behavior using standard pressure-area isotherm measurements and x-ray diffraction. The isotherm was measured using a compression rate of $4 \text{ cm}^2/\text{min}$. The resulting surface pressure versus surface area curve is shown in Fig. 1 for a case of $21 \text{ }^\circ\text{C}$ on a pH 2.5 surface. The kink at a surface pressure of $\Pi = (26.8 \pm 0.5) \text{ mN/m}$ indicates the transition from the L_2 to the L_2' phase (see x-ray data). The kink is sharp, and there is no evidence of any unusual phase behavior in the isotherm. This was typical of all the isotherms that were measured.

GIXD measurements were performed to elucidate the 2D symmetry of the chain lattices on the \AA -scale. Figure 2 shows selected contour plots of the diffracted intensities at different lateral pressures. Starting at low pressures, the monolayer exhibits two low-order diffraction peaks, the degenerate $(1, \pm 1)$ reflection above the horizon and the non-degenerate $(0, 2)$ reflection at zero Q_z indicative for a centered rectangular chain lattice.

The chains are tilted in the direction towards nearest neighbors (NN) along the short axis of the orthorhombic in-plane unit cell. The lattice is distorted from hexagonal packing in NN direction ($Q_{xy}^n > Q_{xy}^d$), where Q_{xy}^n is the maximum position of the non-degenerate peak. On increasing pressure, a transition to an NNN-tilted phase has been observed. This phase is characterized by an intensity distribution with two diffraction peaks at non-zero Q_z -values with $Q_z^n = 2 \cdot Q_z^d$ ¹². Surprisingly, the transition is not characterized by a well-defined transition pressure but occurs over a certain pressure range. In this transition range, four Bragg peaks corresponding to two rectangular lattices with different tilt azimuth can be seen. This corresponds to the range of pressures in Fig. 3a where no data is plotted. Recall, the kink in the isotherm corresponds to the starting point of this transition range. But, there is no evidence for the phase coexistence in the isotherm data or in Brewster angle microscope images²². This is an issue that will require further study.

A linear relationship of the square of the tilt order parameter, $\eta^2 = \sin^2(t)$, versus the lateral pressure is expected for a second order transition, where η is proportional to $(\pi_0 - \pi)^{1/2}$ and π_0 is the tilting transition pressure¹². The linear relation is also observed for $1/\cos(t)$ versus the lateral pressure. This follows from the simplest approximation which assumes that the packing of the chains in the cross-section normal to the chains remains unchanged in the condensed state independent of the phase structure²³. Figure 3a displays such a linear dependence for the monolayer on the subphase with pH 2.5 at two different temperatures. In both cases, the tilt angle decreases monotonically as the surface pressure is increased, with no discontinuities at the phase transition. The value of the tilting transition pressure obtained from the extrapolation to zero tilt decreases with decreasing temperature. At 21 °C, the transition to the non-tilted S phase is expected at

approximately $79 \text{ mN}\cdot\text{m}^{-1}$ while the transition pressure at $5.6 \text{ }^\circ\text{C}$ is much lower ($68 \text{ mN}\cdot\text{m}^{-1}$). Using water as a subphase also decreases this transition pressure ($66 \text{ mN}\cdot\text{m}^{-1}$ at $21 \text{ }^\circ\text{C}$).

For symmetry reasons, the L_2 phase was subdivided into two phases, L_{2d} and L_{2h} , possessing disordered and herringbone-ordered backbone planes, respectively. Plotting the signed unit cell distortion $d = (l_1^2 - l_2^2)/(l_1^2 + l_2^2) \cdot \cos 2(\beta - \omega)$, where l_1 and l_2 are the major and minor axes of the ellipse passing through all six nearest neighbors of a hydrocarbon chain, and β and ω are the tilt and distortion azimuths, respectively, as a function of $\sin^2(t)$, a linear relation is expected according to the Landau theory prediction^{12,24}. The data taken on water and a subphase with pH 2.5 but at the same temperature lie on the same straight line (Figure 3b) indicating that the monolayer forms the same type of phases on these subphases. Decreasing the temperature shifts this line almost parallel. The extrapolation to zero tilt yields a d_0 value, which gives information about the different contributions to the distortion (chain tilt, backbone ordering). The observed d_0 values amount to -0.11 at $21 \text{ }^\circ\text{C}$ and to -0.14 at $5.6 \text{ }^\circ\text{C}$ indicating an effect of backbone ordering, which increases with decreasing temperature. The values are similar to the ones observed for behenic acid²⁵.

As one can see from Fig. 3b, the distortion of the unit cell passes through zero. In the case of behenic acid, the undistorted lattice has been observed within the L_{2h} phase where the distortion azimuth changes from NN to NNN on increasing pressure. At the transition to the L_2' both the tilt and distortion direction change (tilt from NN to NNN and distortion from NNN to NN). In our case, we did not observe any change of distortion direction within the pure L_{2h} phase (all the time NN tilt and NN distortion). On

compression, the distortion is zero at a particular lateral pressure where there is the overlapping of two diffraction patterns (L_{2h} and L_2'). Estimating the tilt angle at which the lattice is undistorted leads to a lateral pressure of $37 \text{ mN}\cdot\text{m}^{-1}$ at $21 \text{ }^\circ\text{C}$ and $23 \text{ mN}\cdot\text{m}^{-1}$ at $5.6 \text{ }^\circ\text{C}$ on a subphase with pH 2.5. On water, this pressure amounts to $31 \text{ mN}\cdot\text{m}^{-1}$ at $21 \text{ }^\circ\text{C}$. At higher temperatures, this pressure is almost in the middle of the observed coexistence range, whereas it is almost at the end of the coexistence range at lower temperatures.

The results of the oscillatory experiments are plotted in Fig. 4 for pH 2.5 at $21 \text{ }^\circ\text{C}$. The dependence of the elastic component of the shear modulus, G' , versus pressure and the viscous component, G'' , versus pressure for three different values of frequency are plotted. There are two striking features of the results: the peak in response as a function of pressure and the independence of the peak on frequency. Figure 5 shows measurements of G' and G'' as a function of pressure for three different temperatures on a subphase of pH 5.6 water. This illustrates the strong temperature dependence of the peak. In all of the measurements, one observes three general regions of behavior. Focusing on the case in Fig. 4 (which corresponds to the isotherm shown in Fig. 1), there is a change in slope of the viscoelastic response at a pressure consistent with the initial phase transition to the L_2' phase. But, the peak in viscosity does not correspond to any feature in the isotherms; however, it is coincident with the pressure at which the x-ray data indicates that the hexagonal lattice is undistorted. Finally, one observes the transition to what is most likely the S phase. This is based on comparisons with measurements of the complex shear modulus in heneicosanoic acid at lower temperatures⁸.

For comparison with the x-ray data, the temperature dependence of the peak pressure is useful. Figure 6 is a graph of the pressure at which the peak occurs as a function of temperature for three different cases: the original sample on pH 2.5 water at 21 °C, a series of data on pH 5.6 water, and measurements taken with a new sample on pH 2.5 water. The data for pH 5.6 is sufficiently linear that one can use it to extrapolate to the lower temperatures, and the line in Fig. 6 is a fit to the data that is used for such an extrapolation. It is worth commenting on the disagreement between the two different pH 2.5 measurements near 21 °C. These measurements were made with different samples. It should be noted that not only was the pressure at which the peak viscosity occurred was shifted, but the other features of the curve corresponding to the various phase transitions were also shifted in a consistent manner. This suggests a systematic error due to impurities in the samples. Therefore, since the initial pH 2.5 viscosity data had good agreement for the onset of the L_2' phase between the isotherms, viscosity measurement, and x-ray data, we will focus on these data for comparison with the x-ray results.

4. Discussion

We have shown clear evidence for a peak in the flow response of the monolayer 2-OH TCA at a pressure of $40 \text{ mN}\cdot\text{m}^{-1}$ on subphase with a $\text{pH} = 2.5$. This peak is observed to occur in both the viscous and elastic response of the material and is independent of the applied frequency. This peak appears to correspond to the complete disappearance of the L_{2h} phase, as determined by x-ray measurements. As an additional test of this correspondence, it is worth comparing the data on pH 5.6 and the temperature dependence of the transitions. First, the x-ray data shows a transition to an undistorted hexagonal lattice on water at $31 \text{ mN}\cdot\text{m}^{-1}$ at 21 °C. This is very different from the

observed end of the coexistence on water at $40 \text{ mN}\cdot\text{m}^{-1}$ at $21 \text{ }^\circ\text{C}$. For pH 5.6 at $21 \text{ }^\circ\text{C}$, the peak in viscosity is observed to occur at $37 \pm 2 \text{ mN}\cdot\text{m}^{-1}$. This favors a correlation between the peak and the complete disappearance of the L_{2h} phase. As a check on the measurements, one can extrapolate the location of the peak to the lower temperature. In this case, the x-ray data does not distinguish the undistorted lattice and the complete disappearance of the L_{2h} phase, as they both are observed at $23 \pm 1 \text{ mN}\cdot\text{m}^{-1}$. The peaks in the response moduli of the monolayer do extrapolate to $23 \pm 2 \text{ mN}\cdot\text{m}^{-1}$ at $5.6 \text{ }^\circ\text{C}$ on water. This demonstrates the consistency between the temperature dependence of the structure, as determined by the x-ray measurements, and the temperature dependence of the rheological properties of the monolayer.

There are two features of the behavior of 2-OH TCA that raise interesting questions. First, the phase behavior of 2-OH TCA is different from that observed for simple fatty acids. In the case of fatty acids the same phase sequence ($L_{2h} - L_2' - S$) was found but with defined transition pressures between the phases. Here we found a pressure range for the coexistence of L_{2h} and L_2' , which is difficult to understand in terms of equilibrium thermodynamics. However, the x-ray intensity distribution shows clearly that the transition range between the NN tilted and NNN tilted state is not characterized by the appearance of an intermediate phase with intermediate tilt (oblique in-plane lattice) as observed in a mixture of stearyl-rac-glycerol and 12-hydroxy-stearyl-rac-glycerol²⁶. The appearance of the transition range seems to be a kinetic phenomenon due to the chemical structure of the molecule. The cross sectional area of the chains amounts to 19.5 \AA^2 at $21 \text{ }^\circ\text{C}$ and 19.2 \AA^2 at $5.6 \text{ }^\circ\text{C}$ and indicates an increase in chain packing with decreasing temperature. To exclude the effect of tilt, we have calculated the unit cell

parameters a_p and b_p in the plane normal to the long axes of the molecules. Comparing these data with the literature data of many different monolayers¹² shows that the packing at low temperature and low pressure (L_{2h} phase) is a pseudo-herringbone packing (PHB) with $a_p = 4.304 \text{ \AA}$ and $b_p = 8.937 \text{ \AA}$. The PHB motif should have an angle of 40° between the backbone planes of the chains. In the L_2' phase at high pressure, the packing is a herringbone (HB) arrangement with $a_p = 5.062 \text{ \AA}$ and $b_p = 7.577 \text{ \AA}$ ^{27,28}. These values increase to 5.02 \AA and 7.75 \AA at $21 \text{ }^\circ\text{C}$. On increasing pressure, the packing changes from PHB to HB. Having a closer look on the diffraction patterns, the transition from L_{2h} to L_2' is characterized by an unusual behavior. At $21 \text{ }^\circ\text{C}$, L_{2h} and L_2' coexist over a larger pressure range (between $27 \text{ mN}\cdot\text{m}^{-1}$ and $40 \text{ mN}\cdot\text{m}^{-1}$) above the kink in the isotherm. Decreasing temperature decreases this pressure range drastically. At $5.6 \text{ }^\circ\text{C}$, the coexistence of both phases is seen between approximately $15 \text{ mN}\cdot\text{m}^{-1}$ and $22 \text{ mN}\cdot\text{m}^{-1}$. This shows that the coexistence of phases is a kinetic phenomenon. It is interesting to note that at the beginning of the phase coexistence range a L_2' phase with NNN tilt and NNN distortion is found, which was not described before. Further compression leads to a change in the distortion azimuth to NN via an undistorted lattice. This shows that the usually observed jump in distortion azimuth at the $L_{2h} - L_2'$ transition is replaced by a continuous change, which occurs in the L_2' instead in the L_{2h} phase observed for many amphiphiles¹². Figure 7 displays the change in the diffraction pattern with time after expansion of the compressed monolayer (L_2') to $15 \text{ mN}\cdot\text{m}^{-1}$. The formation of the new phase, either L_2' on compression or L_{2h} on expansion, is kinetically hindered because of the specific interaction due to the special chemical structure.

The other issue is the peak in the flow response as a function of pressure. The nature of this peak also appears to be different from that in fatty acids. At 21 °C, the pressure of the peak in the flow response ($40 \text{ mN}\cdot\text{m}^{-1}$) is connected with the complete disappearance of the L_{2h} phase. Measurements as a function of pH and temperature confirm this picture, and strongly suggest the source of the peak is more closely related to the behavior of the tilt of the chains, as suggested for fatty alcohols. (However, it should be noted that for the fatty alcohols, there was no evidence of any correspondence with a phase transition.) Other differences exist between the observed peak for 2-OH TCA and C21. For 2-OH TCA, the peak is apparent in both the elastic and the viscous response. For fatty acids, the peak was predominately observed for the viscous response. Finally, the variation in the flow properties is much larger, spanning orders of magnitude.

The richness of the observed rheological and phase behavior presents an interesting theoretical and experimental challenge that could potentially provide significant insight into the interaction between mesoscopic and microscopic structure as it relates to the determination of macroscopic flow properties. The clarification of mechanisms that produce peaks in the rheological properties of complex fluids is an important problem. Also, the question of coexistence of phases remains an interesting one, especially the indications that this is a kinetic effect.

ACKNOWLEDGEMENTS: We thank G. Fuller and C. Knobler for useful discussions. M. Twardos and M. Dennin thank NSF grant CTS-0085751 for funding. They also thank the Research Corporation and Sloan Foundation for additional funding. We thank HASYLAB at DESY, Hamburg, Germany, for beam time and providing excellent facilities and support. The help of Kristian Kjaer with setting up the x-ray experiment is gratefully acknowledged.

Figure captions

Figure 1. Measured isotherm for 2-OH- TCA on pH 2.5 substrate.

Figure 2. Selected contour plots of the corrected x-ray intensities versus in-plane and out-of-plane scattering vector components Q_{xy} and Q_z at 5.6 °C on a subphase with pH 2.5. The results obtained at 0.9, 16 and 41 mN·m⁻¹ (from left to right) are shown.

Figure 3a. $\sin^2(t)$ as function of the lateral pressure π for 2-OH TCA on a subphase with pH 2.5 at 21 °C (●) and at 5.6 °C (■). The linear extrapolation towards zero tilt angle yields the pressure π_t of the tilting transition.

Figure 3b. Signed unit-cell distortion d versus $\sin^2 t$ for 2-OH TCA on water (▲) and on pH 2.5 (●) at 21 °C as well as on pH 2.5 at 5.6 °C (■). At 21 °C, the data contribute to a common regression line indicating that the monolayer structures are the same on these two subphases.

Figure 4a. Measurement of $G'(\omega)$ as a function of surface pressure for three different values of ω : $\omega = 0.314$ rad/s (+); $\omega = 0.157$ rad/s (O); and $\omega = 0.063$ rad/s (▲).

Figure 4b. Measurement of $G''(\omega)$ as a function of surface pressure for three different values of ω : $\omega = 0.314$ rad/s (+); $\omega = 0.157$ rad/s (O); and $\omega = 0.063$ rad/s (▲).

Figure 5a. Measurement of $G'(\omega)$ as a function of surface pressure for three different temperatures on a pure water subphase. There is a clear shift in the peak with temperature.

Figure 5b. Measurement of $G''(\omega)$ as a function of surface pressure for three different temperatures on a pure water subphase. The shift in the peak with temperature is clear.

Figure 6. Plot of the peak value of the rheological response as a function of temperature for three different conditions: pH 5.6 water (\blacktriangle), initial studies using pH 2.5 water (\bullet), and later studies using pH 2.5 water (Δ).

Figure 7. 3D plot of the corrected x-ray intensity as a function of the in-plane and out-of-plane scattering vector components Q_{xy} and Q_z at 5.6 °C on a subphase with pH 2.5 directly after expansion to 15 mN·m⁻¹ (left) and after waiting 75 min at 15 mN·m⁻¹ (right). The disappearance of the scattering from the L₂' phase is clearly visible.

References

- (1) Kurnaz, M. L.; Schwartz, D. K. *Physical Review E* **1997**, *56*, 3378.
- (2) Ivanova, A.; Kurnaz, M. L.; Schwartz, D. K. *Langmuir* **1999**, *15*, 4622.
- (3) Ivanova, A. T.; Schwartz, D. K. *Langmuir* **2000**, *16*, 9433.
- (4) Maruyama, T.; Fuller, G.; Frank, C.; Robertson, C. *Science* **1996**, *274*, 233.
- (5) Iñes-Mullol, J.; Schwartz, D. K. *Langmuir* **2001**, *17*, 3017.
- (6) Iñes-Mullol, J.; Schwartz, D. K. *Nature* **2001**, *410*, 348.
- (7) Abraham, B. M.; Miyano, K.; Xu, S. Q.; Ketterson, J. B. *Physical Review Letters* **1983**, *51*, 1975.
- (8) Ghaskadvi, R. S.; Ketterson, J. B.; Dutta, P. *Langmuir* **1997**, *13*, 5137.
- (9) Ghaskadvi, R. S.; Dennin, M. *Langmuir* **2000**, *16*, 10553.
- (10) Brooks, C. F.; Fuller, G. G.; Frank, C. W.; Robertson, C. R. *Langmuir* **1999**, *15*, 2450.
- (11) Knobler, C. M.; Desai, R. C. *Annual Review of Physical Chemistry* **1992**, *43*, 207.
- (12) Kaganer, V. M.; Möhwald, H.; Dutta, P. *Rev. Mod. Phys.* **1999**, *71*, 779
- (13) Edwards, D. A.; Brenner, H.; Watson, D. T. *Interfacial Transport Processes and Rheology*; Butterworth-Heinemann: Boston, 1991.
- (14) Ivanova, A. T.; Iñes-Mullol, J.; Schwartz, D. K. *Langmuir* **2001**, *17*, 3406.
- (15) Ghaskadvi, R. S.; Carr, S.; Dennin, M. *Journal of Chemical Physics* **1999**, *111*, 3675.

- (16) Copeland, L. E.; Harkins, W. D.; Boyd, G. E. *Journal of Chemical Physics* **1942**, *10*, 357.
- (17) Ghaskadvi, R. S.; Dennin, M. *Review of Scientific Instruments* **1998**, *69*, 3568.
- (18) Stone, H. A. *Physics of Fluids* **1995**, *7*, 2931.
- (19) Macosko, C. W. *Rheology Principles, Measurements, and Applications*; VCH Publishers: New York, 1994.
- (20) Jacquemain, D.; Leveiller, F.; Weinbach, S.; Lahav, M.; Leiserowitz, L.; Kjaer, K.; Als-Nielsen, J. *Journal American Chemical Society* **1991**, *113*, 7684.
- (21) Als-Nielsen, J.; Jacquemain, D.; Kjaer, K.; Leveiller, F.; Lahav, M.; Leiserowitz, L. *Physics Reports* **1994**, *246*, 252.
- (22) Knobler, C. M., private communication, 2003.
- (23) Bringezu, F.; Dobner, B.; Brezesinski, G. *Chem. Eur. J.* **2002**, *8*, 3203.
- (24) Kaganer, V. M.; Loginov, E. B. *Physical Review E* **1995**, *51*, 2237.
- (25) Kenn, R. M.; Böhm, C.; Bibo, A. M.; Peterson, I. R.; Möhwald, H.; Als-Nielsen, J.; Kjaer, K. *Journal of Physical Chemistry* **1991**, *95*, 2092.
- (26) Krasteva, N.; Vollhardt, D.; Brezesinski, G. *J. Phys. Chem. B* **2000**, *104*, 8704.
- (27) Kitaigorodski, A. I. In *Organic Chemical Crystallography*; Consultants Bureau: New York, 1961.
- (28) Kuzmenko, I.; Kaganer, V. M.; Leiserowitz, L. *Langmuir* **1998**, *14*, 3882.

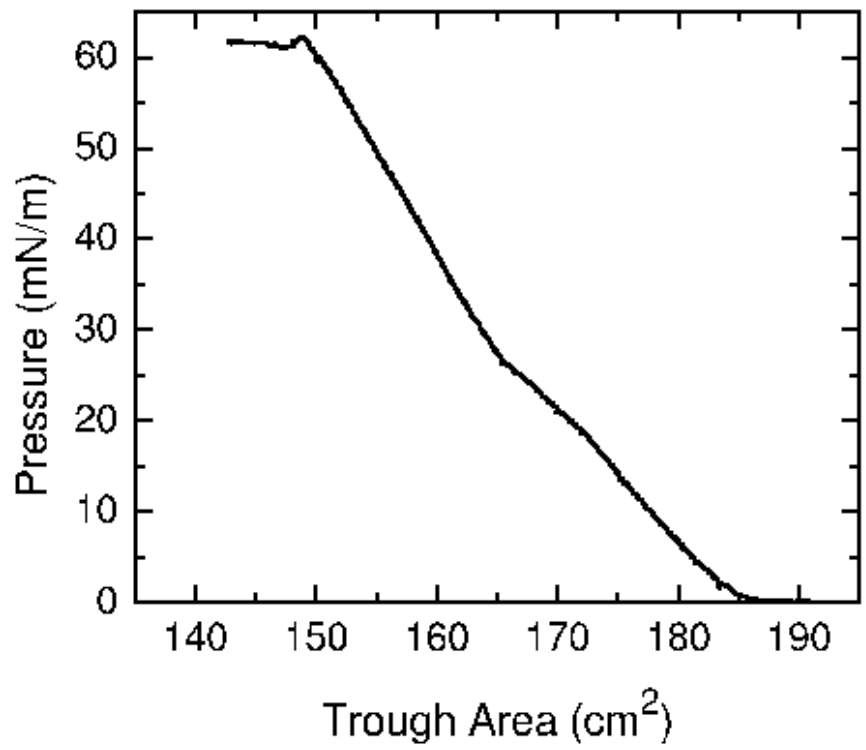


Figure 1: Twardos, et al.

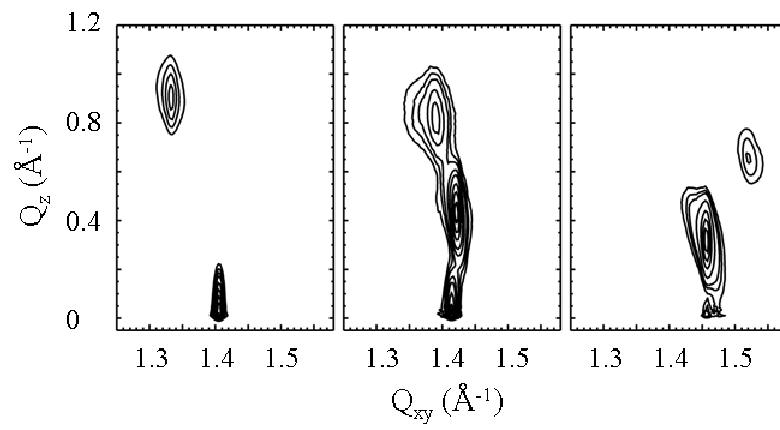
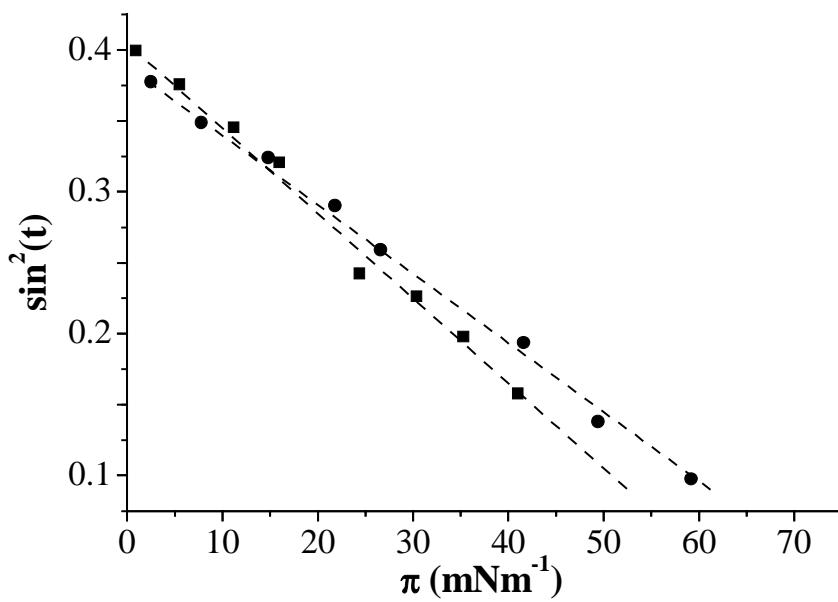
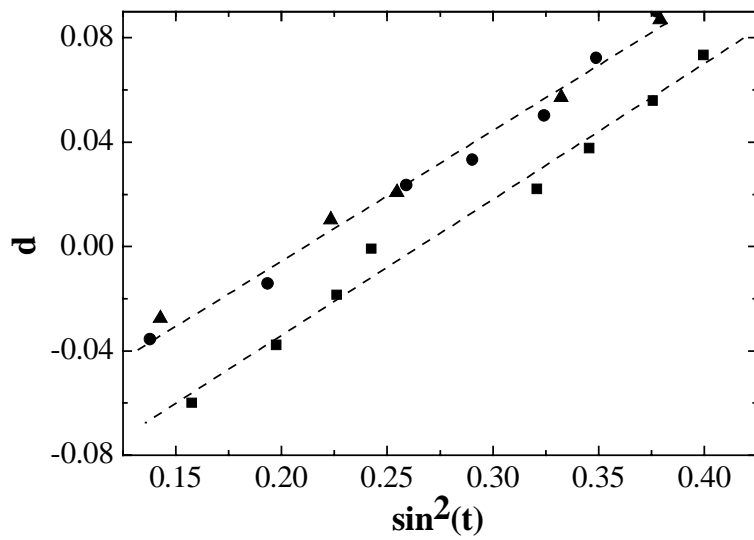


Figure 2



a



b

Figure 3

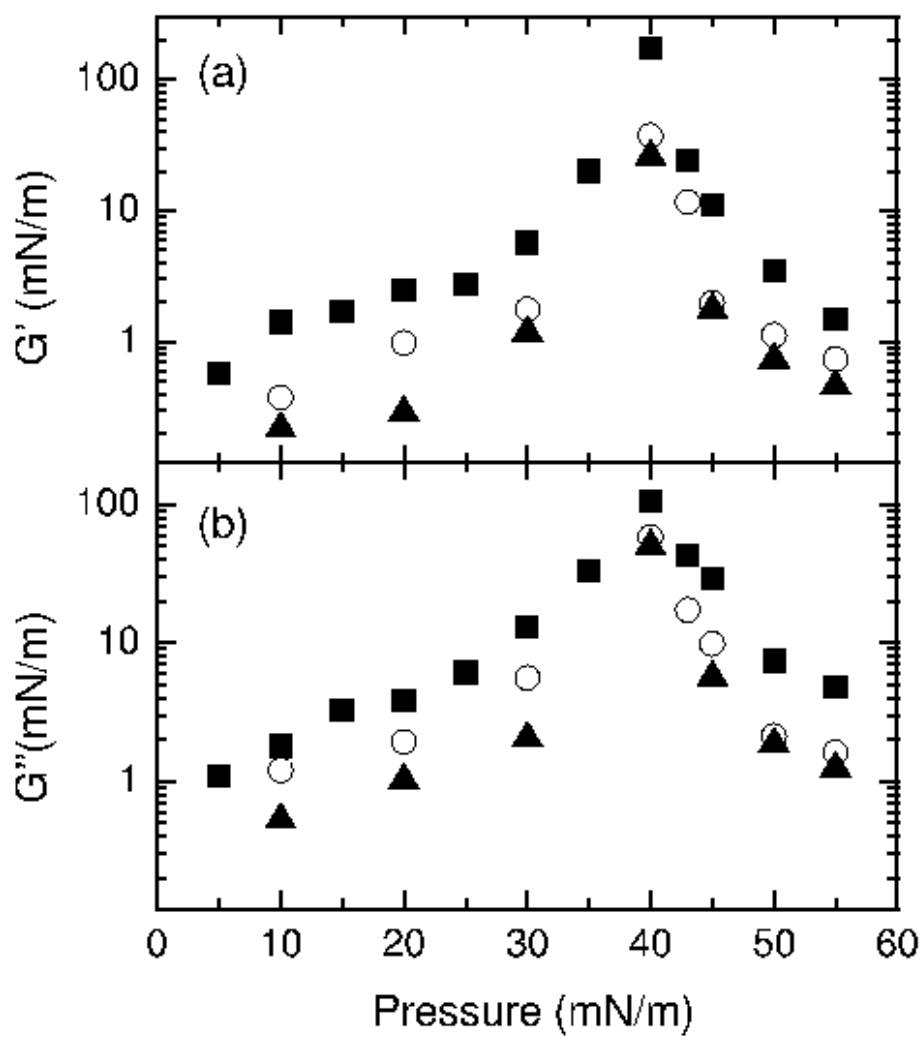


Fig. 4 Twardos, et al.

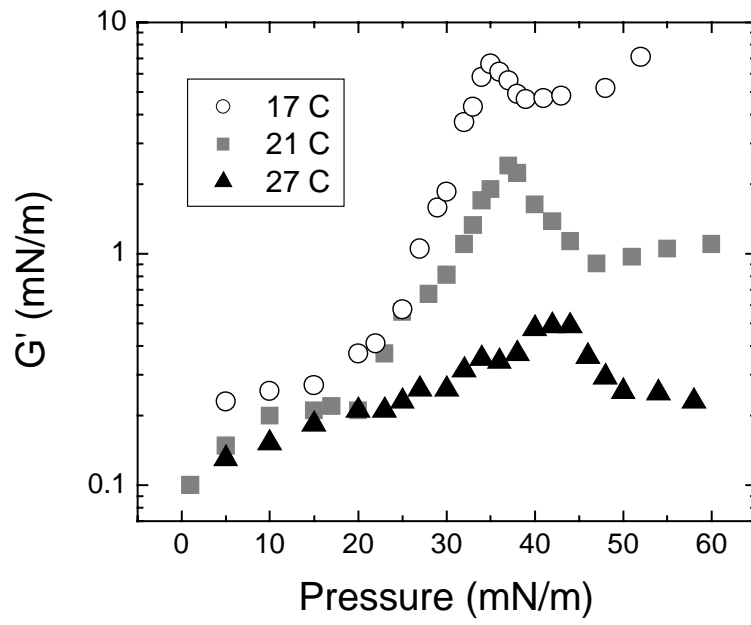


Figure 5a

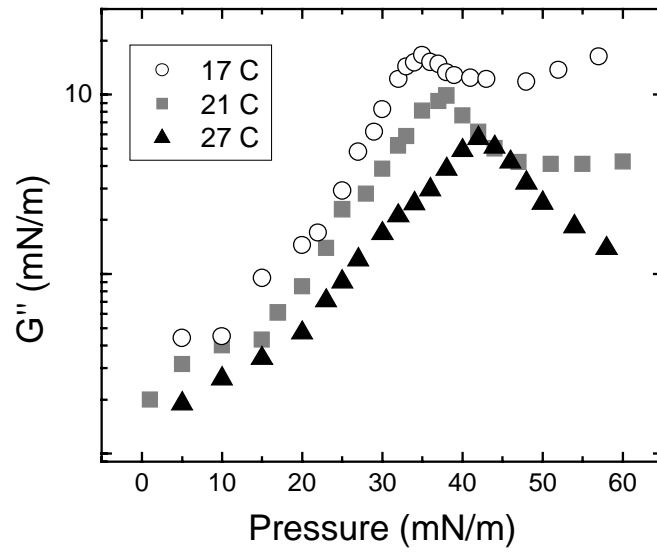


Figure 5b

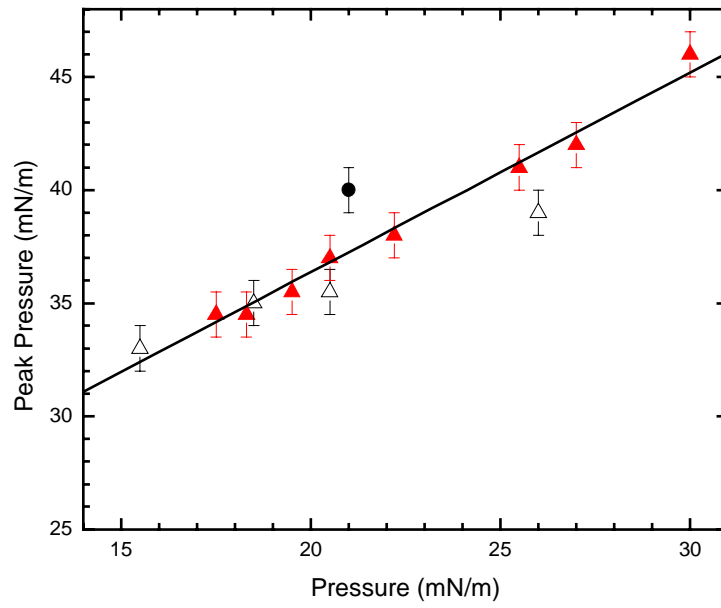


Figure 6

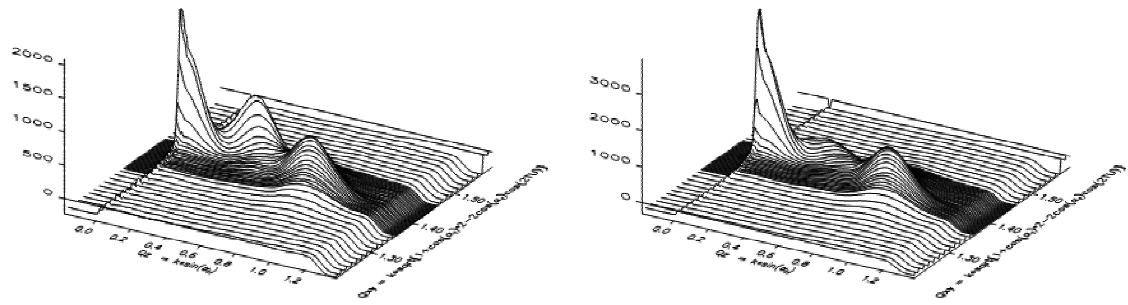


Figure 7